12/11/12/91 8S (1)

MORGANTOWN ENERGY TECHNOLOGY CENTER

DOE/METC-91/4106
(DE91002080)

Rapid Sulfur Capture Studies at High Temperatures

Technical Note

By
G.A. Richards
W.F. Lawson
D.J. Maloney
D.W. Shaw

December 1990

U.S. DEPARTMENT OF ENERGY
OFFICE OF FOSSIL ENERGY
MORGANTOWN ENERGY TECHNOLOGY CENTER
MORGANTOWN, WEST VIRGINIA

DISCLAIMER

DOE/METC--91/4106

DE91 002080

Rapid Sulfur Capture Studies at High Temperatures

Technical Note

By
G. A. Richards
W. F. Lawson
D. J. Maloney
D. W. Shaw

U.S. Department of Energy
Office of Fossil Energy
Morgantown Energy Technology Center
P.O. Box 880
Morgantown, West Virginia 26507-0880

December 1990

Acknowledgment

The authors wish to acknowledge outstanding suggestions, experimental operation, and technical support from Mr. Rick Griffith and Mr. Keith Dodrill. Assorted contributions from other members of METC's Test Operations Branch are gratefully acknowledged, including Mr. Randy Carter and Mr. Dick Loomis.

Contents

List of Figures

List of Tables

1.0 Introduction

Recent work by Abichandani, Chatwani, and Stickler (1989) and Bannister et al. (1990) has suggested that it may be possible to capture sulfur using limestone sorbents at high temperatures and short residence times. These results appear to stand in marked contrast to earlier studies that attempted to capture sulfur on limestone in flames but yielded only marginal performance. Conventional thinking attributes the low sulfur capture in those studies to the high flame temperatures, which generally exceeded the temperature for a stable equilibrium product from the limestone-sulfur reactions. Also, high flame temperatures can promote particle sintering, such that little surface area is available for sulfur access to the sorbent.

Even when temperatures are low enough for a stable limestone-sulfur product to form, basic limitations on sorbent surface area and pore plugging have generally prevented utilization from approaching theoretical limits. Borgwardt (1985) has shown that rapid heating of limestone produces a sorbent with a large surface area, which should be better able to capture sulfur. One might extrapolate that the highest heating rates should give the largest surface area, and so higher temperatures would favor the generation of a sorbent with a large available surface area. While the higher temperatures might provide favorable surface areas, the high sorbent temperatures would preclude the formation of a stable equilibrium product.

Abichandani, Chatwani, and Stickler (1989) suggested that it may be possible to capitalize on the benefits of rapid heating rates by utilizing the transient nature of particle heating to capture sulfur during the fleeting moments when the particle is heating and calcining. Because calcination is endothermic, the particle temperature remains low enough to capture sulfur.

Calculations carried out by Lawson et al. (1990) showed that this scenario is possible under idealized conditions. If possible in practice, the proposed behavior would lead to transient sulfur capture on the sorbent particles, at gas temperatures above the point at which equilibrium would predict any stable product. This behavior has been described as "super-equilibrium sulfur capture" or "rapid sulfur capture." The transient nature of the super-equilibrium process requires a strategy either to quench the hot sorbent or possibly to react the sorbent with coal slag, where a host of mineral reactions might be available to stabilize the sulfur products. This latter possibility would be particularly valuable for a slagging combustor using impact separation, where the reacting sorbent could be rapidly transferred to the slag bath below. This strategy has generated considerable interest in the super-equilibrium process and has motivated continuing investigation of the super-equilibrium process for coal-fired turbine combustors (Lawson et al. 1990).

In an effort to confirm the super-equilibrium concept in an independent experiment, this report describes sulfur capture studies conducted in a simulated gas turbine environment at temperatures, pressures, residence times, and sulfur levels representative of an operating turbine system. METC's Gas Turbine Research Combustor (GTRC) was modified specifically for these tests. Rather than systematically varying the parameters, data were first collected to

determine conditions that would reproduce the super-equilibrium behavior. No attempt was made to extract kinetic data for calcination or sulfur capture, as might be done in a comprehensive study of sorbent behavior. While some interesting anomalies are present in the calcination data and in the limited surface area data, no attempt was made to pursue those issues. Since little sulfur capture was observed at operating conditions where "super-equilibrium" might be expected to occur, tests were stopped when the wide range of parameters that were studied failed to produce significant sulfur capture via the super-equilibrium mechanism.

Considerable space in this report is devoted to a description of the experiment, including details of the GTRC construction. This description is included because we have received requests for a detailed description of the GTRC itself, as well as the pressurized dry powder feed system. In addition, many questions about accurately sampling the sulfur species from a high-temperature, high-pressure reactor were raised during the course of this investigation. A full account of the development of the gas and particulate sampling train is thus provided.

2.0 GTRC Overview

2.1 Combustor Body

The major component of the GTRC is the combustor body itself. Figure 1 shows a cutaway view of the jet-stirred and plug-flow combustion zones. The combustor interior consists of a 20.3-cm (8-in) diameter, spherical chamber coupled to a 7.6-cm (3-in) diameter tube. Access ports enter the jet-stirred zone for optical access, fuel injection, or particulate injection, depending on the specific use of the combustor. The combustor interior was formed from castable refractory (Plicast type K-L, Pilbrico Company) poured around plastic and sheetmetal forms. The pressure vessel was constructed from 45.7-cm (18-in) class 300, 316 stainless steel flanges and hemispherical end caps, with the bottom cap modified to accept the plug-flow connection. The flange halves mate at a 45-degree angle from the horizontal so that the ports enter on the same horizontal plane. This arrangement also allows service access to the combustor interior by simply unbolting the main flanges. The plug-flow zone was fabricated from 20.3-cm (8-in) stainless steel pipe using class 300 flanges. The plug-flow section was fitted with a water cooling jacket, manufactured from rolled sheet metal, and welded to the exterior of the section. Gases exit the plug-flow zone from a tee section located 66 centimeters (26 inches) below the bottom of the jet-stirred zone.

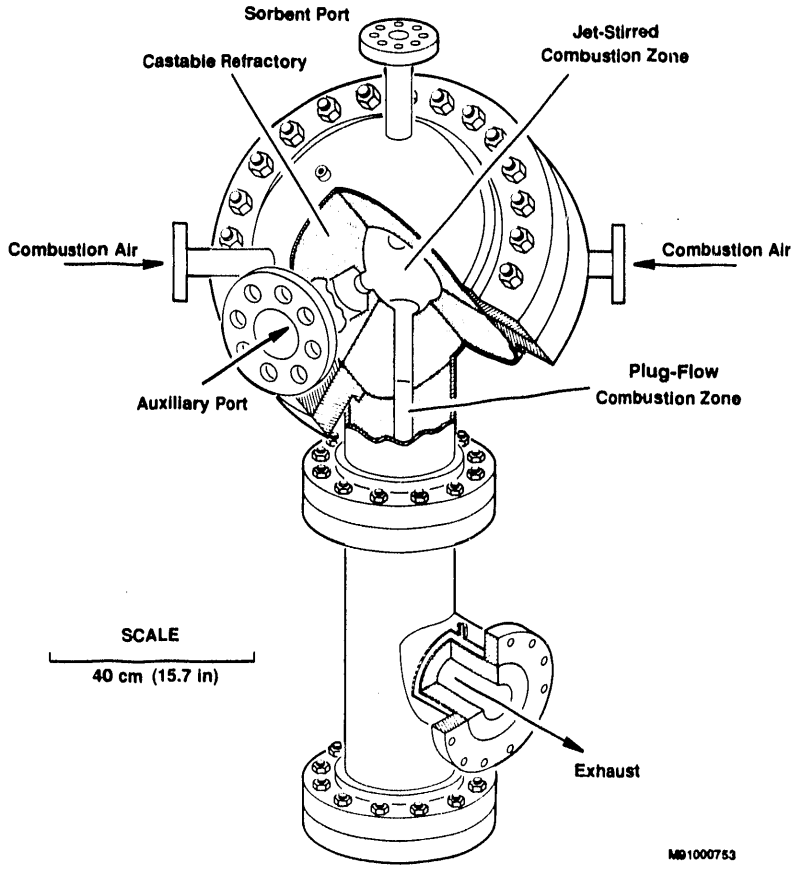

Figure 1. Overview of the Gas Turbine Research Combustor (GTRC)

2.2 Combustor Zones

A detailed layout of the combustor zones is shown in Figure 2. The jet-stirred region of the combustor was designed for flexible adaptation to a number of planned research projects:

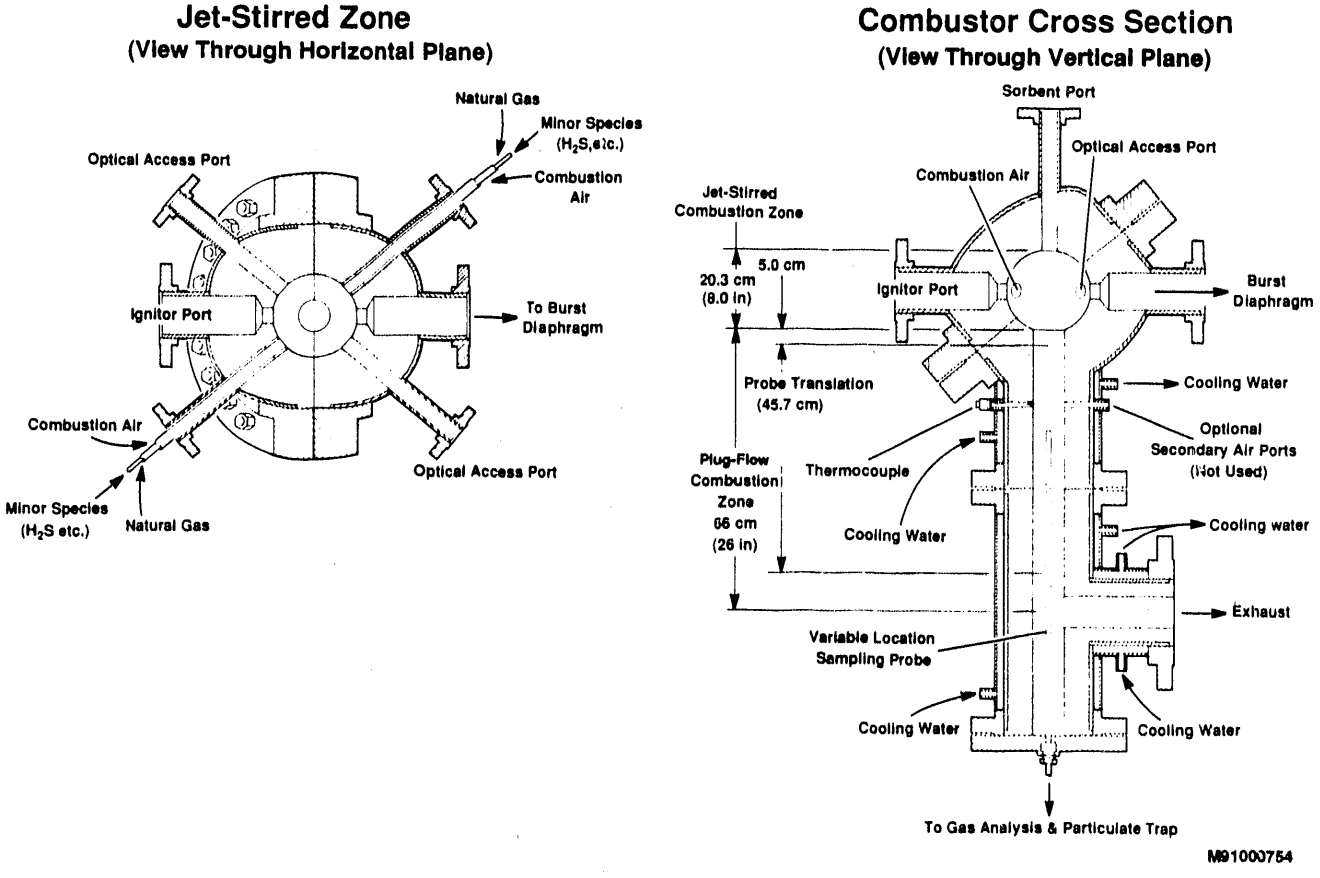

Figure 2. Details of Combustor

coal-water slurry, coal gases, and sulfur sorbent utilization. Thus, the ignitor port and burst diaphragm port were fitted with oversized 10.2-cm (4-in) flanges and passages that narrowed to a 2.5-cm (1-in) opening into the combustor interior. These relatively large openings were used for coal-slurry nozzles in earlier tests.

In the sulfur study, these large ports were fitted with formed refractory plugs, leaving only a passage for the ignitor and burst diaphragm connection. Ignition was achieved by inserting a torch through a 2.5-cm (1-in) ball valve (not shown) connected to the ignitor port. An optical access port crosses the spherical diameter at a right angle to the combustion air ports. The combustion air is conveyed by a 12.7-mm (0.5-in) tube, which runs the length of the port to the combustor interior. Inside this tube, a 9.5-mm (0.375-in) tube conveys natural gas to the combustor. Finally, a 6.4-mm (0.25-in) central tube allows injection of minor gas species, such as hydrogen sulfide (H_2S), which was injected in this sulfur capture study.

The plug-flow zone is outfitted with two opposed secondary air injection ports, as shown in the vertical plane cutaway view (Figure 2). In the sorbent tests, secondary air was not injected; therefore, one port was capped, and the other was used for thermocouple access

only. A 9.5-mm (0.375-in), alumina sheathed, type-R thermocouple monitored the temperature of the plug-flow interior wall. Figure 2 also shows the three separate water jackets, which cool the plug-flow exterior. Sufficient cooling water was run in each section to maintain a cooling water exit temperature of less than 333 K (140 °F).

The plug-flow section can be traversed with the sampling probe during the test. The sampling probe extends to within 5.0 centimeters (2.0 inches) of the bottom of the jet-stirred region and can move 45.7 centimeters (18.0 inches) down from that point. Depending on the flow rates, this allows sampling at plug-flow residence times from 5 to 150 milliseconds or more. The exhaust tee was mated to a 10.2-cm (4-in) pipe, with exterior water cooling to reduce the gas temperature to less than 811 K (1,000 °F) at all operating conditions. A high-temperature backpressure control valve was used to establish the operating pressure.

Sorbent was injected through the 5.0-cm (2-in) port on the top of the jet-stirred zone. A more detailed explanation of the sorbent injection is given in Section 3.2.

2.3 Combustor Assembly

Figure 3 is a photograph of the combustor assembly. The combustor was mounted on an octagonal platform, with a 1.22-m (4-ft) clearance below the platform deck for probe translation and removal. Aluminum plating surrounded the combustor, both above and below the decking, to protect personnel from vessel or fitting failure. Skin temperatures on the pressure vessel and cooling water exit temperatures were continuously monitored with audible alarms to warn of excessive temperatures.

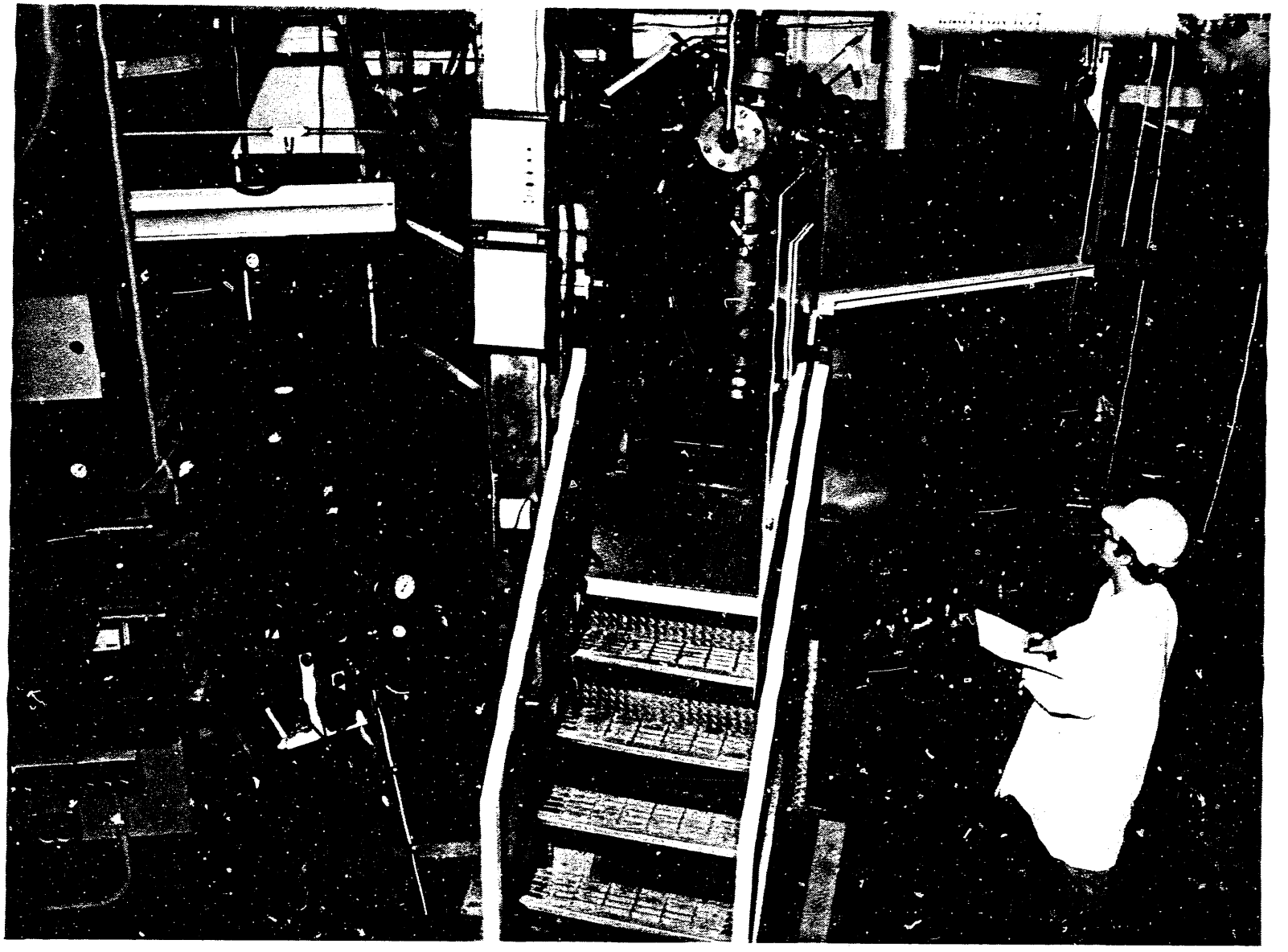

Figure 3. Gas Turbine Research Combustor

3.0 GTRC Experimental Systems

The major experimental systems for the GTRC are the hydrogen sulfide injection system, the sorbent feed system, and the sampling train, which are shown in Figure 4. Flow loops for the combustor gases are measured and controlled with standard valve and orifice run combinations. A detailed description of the less familiar systems is given below.

3.1 Hydrogen Sulfide Injection

To test for sulfur capture, H_2S was injected into the inlet gas stream. (See Figure 2.) Hydrogen sulfide was chosen, rather than sulfur dioxide, because it was gaseous at the test operating pressure. The H_2S was supplied from a condensed liquid storage tank at the vapor pressure of 1,800 kPa (262 psig). Instead of simply metering the vapor phase that left the storage tank at the saturation pressure, the vapor was regulated to 1,500 kPa (220 psia) to prevent condensate from forming in the lines or in the mass flow meter used to control the injection rate. The gas was carried in 6.4-mm (0.25-in) stainless steel lines and metered by a Porter mass flow controller, model 202 fsec. After a test, nitrogen was used to purge all components of the H_2S gas. The purged gases were sent to the combustor before flame extinction to burn all residual H_2S, preventing gas release in the operating area. Hydrogen sulfide alarms continuously monitored the operating area for unsafe H_2S levels caused by inadvertent fitting leaks.

3.2 Sorbent Feed System

It was recognized that accurate metering and steady feeding of the sorbent into the pressurized combustor would be a particularly challenging problem. A literature survey of pressurized feeders and discussions with powder feeding vendors failed to uncover any simple solutions.

The authors are indebted to Mr. Charles Zeh, with METC's Office of Technical Management, who recommended investigating pressurized, dry powder feeders that had been developed under METC's hot-gas cleanup project at Westinghouse Inc., Pittsburgh, Pennsylvania. In a visit to Mr. Gene Smeltzer and Dr. Thomas Lippert at Westinghouse, METC personnel successfully tested the Westinghouse feed concept on our sorbent, leading to subsequent development of a similar feeder at METC.

Figure 4 shows the feed system, which consists of a dry powder feeder mounted inside a pressure vessel. The pressure vessel is constructed from 76.2-cm (30-in), plain steel flanges, pipe, and end caps. The vessel is pressurized with nitrogen almost one atmosphere higher than the combustor so that nitrogen flows steadily from the feed vessel to the combustor. The sorbent is stored in the hopper connected to the feeder, which is a twin-screw, K-Tron, loss-in-weight feeder (model LWFD5-20) with controller K-10S. The twin-screw feature was

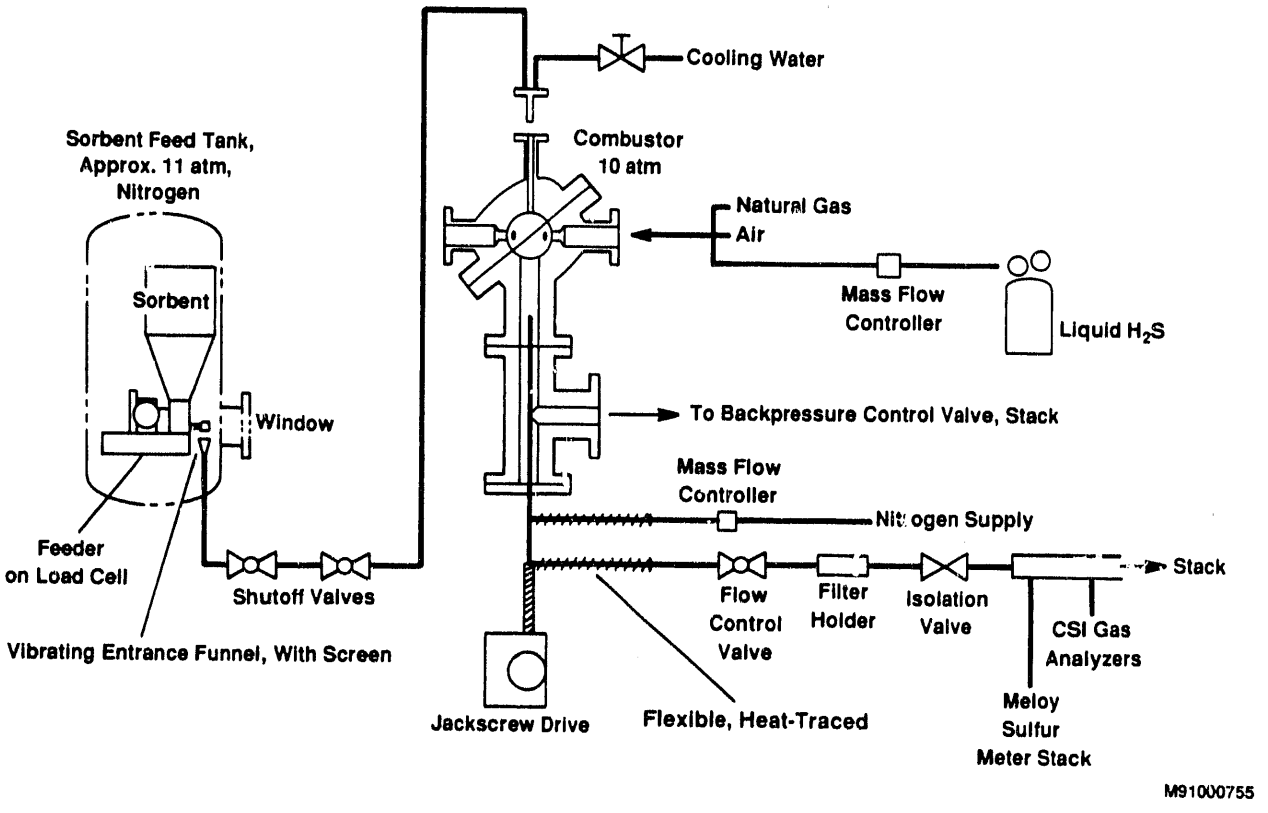

Figure 4. Schematic of Major Experimental Systems

essential to steady feed at low flow rates. The feed rate was monitored via the K-10S controller, which continuously averaged the loss in weight (as measured by the feeder load cell) for a real time measure of the sorbent feed rate. The feed rate was easily changed by the feed screw rpm. The ends of the feeder screws were positioned so that the fed material dropped into a funnel that formed the entrance of the conveying line into the combustor. The conveying line was a 6.4-mm (0.25-in) stainless steel line, with ball valve shutoffs (as shown in Figure 4) to isolate the line or tank during a run. The isolated line could then be purged with high-pressure nitrogen if it clogged during a test.

The feed system was tested by inserting the end of the conveying line into METC's pressurized spray characterization tank, which was operated at 10 atmospheres pressure. Visual observation of the dust exiting the conveying tube initially included unsteady pulses of sorbent. These pulses were the result of small lumps of limestone falling from the end of the feeder screws. This problem was eliminated by placing a 10-mesh screen at a distance of 2 centimeters (0.78 inches) from the top of the funnel. The screen broke up the material so that during steady operation, a fixed supply of sorbent collected on the screen, with the rate of screened material just balancing the supply rate from the feeder screws. The fed sorbent was observed at the end of the conveying line as a steady spray of dust, similar in appearance to a steady spray from a liquid atomizer.

During most of the tests described here, the carrier gas rate feed rate was fixed at 4.25 to 4.75 g/s (450 to 500 scf/h) nitrogen. Figure 4 shows a flanged, water-cooled probe that enters the top of the combustor to inject the sorbent. Details concerning the point of injection into the combustor are discussed in section 4.0.

3.3 Sampling Train

Considerable effort was devoted to developing a sampling train that could accurately monitor sulfur levels from the gas phase and could also produce representative particulate samples. As discussed by Chadaille and Braud (1972), to accurately measure water soluble species, the sample must be maintained at temperatures above the dewpoint along the sample train. Furthermore, Chadaille and Braud show that cooling sufficient to quench reactions of sampled gases can be achieved in just a few centimeters from the tip of a water-cooled probe.

Thus, a sampling probe was designed with a water-cooled tip followed by an insulated section. Rapid gas quench is achieved by convection to the cold metal tip, followed by a relatively constant temperature (above the dewpoint) in the insulated section. The probe was built and excellent sulfur closure was achieved in the absence of sorbent. However, the probe clogged immediately when used with sorbent. Upon disassembly, it was found that a hard plug had formed in the probe tip. The plug was difficult to remove and appeared to be bonded to the metal surface. It is believed that this plugging resulted from water condensation on the cool metal surface capturing the entering sorbent. Thus, even though the mean gas sample temperature was above the dewpoint, the cold boundary layer generated enough moisture condensation to create sampling difficulties.

Because this problem could not be eliminated in a water-cooled quench design, a nitrogen dilution sampling train was used. The sampling train is shown schematically in Figure 4, with more details in Figure 5. Nitrogen diluent is added to the incoming sample at the tip of the probe. The diluent nitrogen (1) cools the sample and stops chemical reactions, (2) lowers the water vapor pressure (meaning a lower dewpoint temperature and less chance for condensing water), and (3) reduces the particulate loading. All these characteristics improve sampling accuracy and reduce the chance of plugging. The drawback is that gaseous concentrations are diluted. Thus, careful control of the dilution rate is essential to accurate gas sampling. This problem was addressed as described in the following paragraphs.

Figure 5 shows how nitrogen is supplied to a mass flow controller and is fed to the probe annulus. All tests were conducted with a probe exit temperature near 488 K (420 °F) and a nitrogen flow rate fixed at 3.3 g/s (350 scf/h).

- Nitrogen flows to the tip of the probe, where an enlarged entrance mixes the nitrogen with some sample gas in the entrance region.

- The mixture then passes down the center tube of the sampling probe.

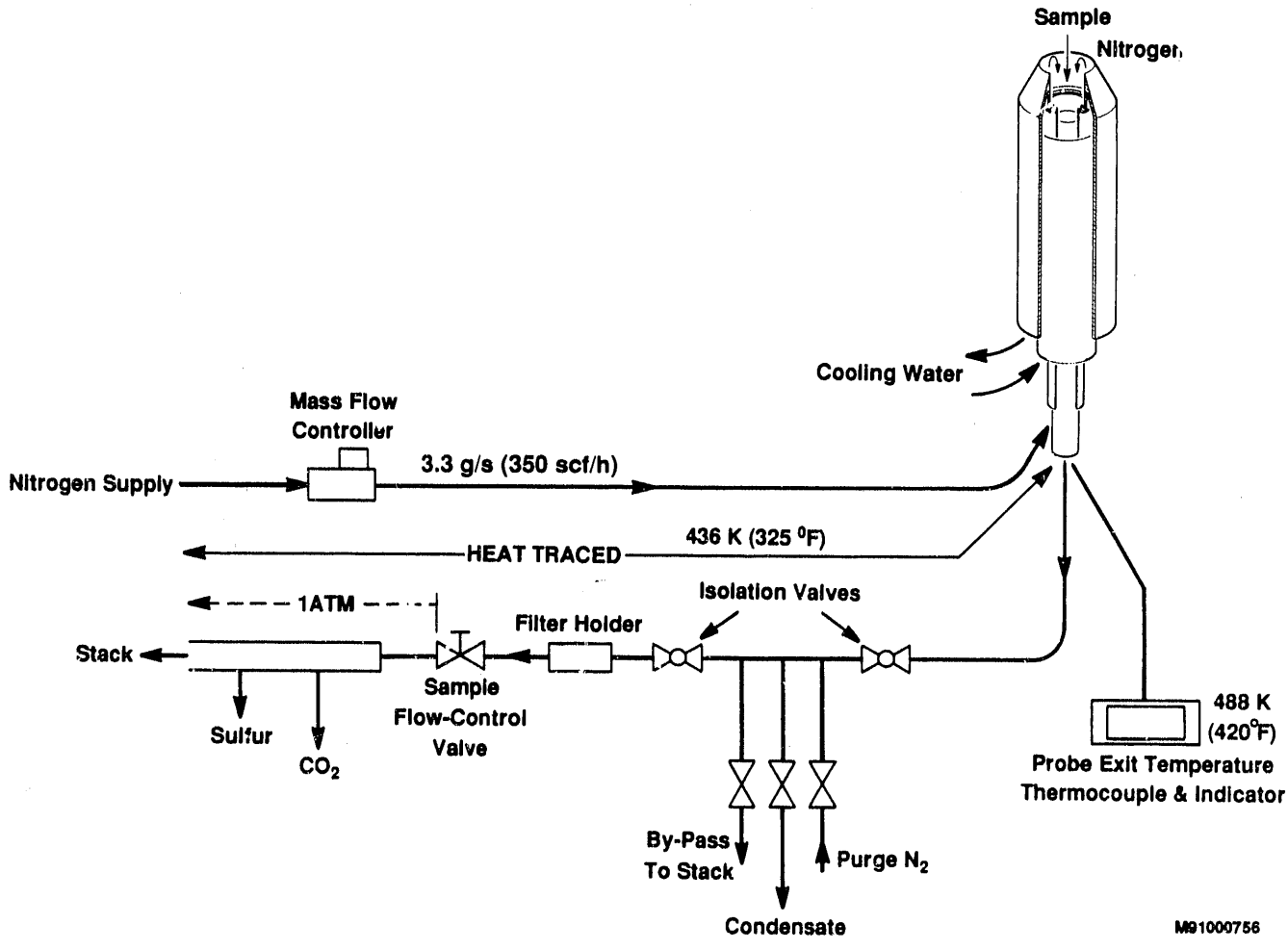

Figure 5. Details of Nitrogen Dilution Sampling Train

- The sample is passed in flexible, heat-traced, 9.53-mm (0.375-in) lines through two isolation valves, a removable particulate filter holder, and then through the sample flow control valve where the pressure is dropped to one atmosphere.

In operation, the dilution rate is established by simply opening the sample flow control valve. Initially, only cold nitrogen will be drawn down the center tube of the sampling probe. As the flow is increased, some combustion gas is also drawn into the system, which is immediately detected by an increased temperature in the probe exit thermocouple. The dilution rate is decreased by increasing the total sample flow at the fixed nitrogen input, i.e., pulling more combustion gas into the probe.

The actual dilution level can be determined in the following manner:

- At a known stoichiometry, the carbon dioxide (CO_2) level in the products of the jet-stirred combustion zone are calculated from the NASA Chemical Equilibrium Code (the CEC code) (Gordon and McBride 1976).

- Because residence times in the jet-stirred zone are on the order of 100 milliseconds, CO_2 levels reach equilibrium values.

- Then, by measuring the actual CO_2 level in the diluted sample and comparing it to the equilibrium value, a dilution ratio for the sample can be calculated.

- Applying this same dilution ratio to the calculated equilibrium value of sulfur species, sulfur closure is checked. Typically, the measured sulfur level was within 5% of the value expected by balancing inlet flows and calculating the dilution level as described.

Obviously, maintaining a constant dilution level was important to accurate testing. During data acquisition, the dilution level could change. For example, if the sample filter partly clogs, the effect would be similar to closing the sample flow control valve and, therefore, increasing the dilution rate (Figure 5). While such behavior would not affect the particulate sample, it would produce an apparent reduction in sulfur level. In practice, clogged filters were easily detected on-line, because the probe exit temperature dropped immediately. Thus, by continuously monitoring the probe exit temperature, it was possible to verify that measured, gas-phase sulfur reductions were not the result of changing dilution ratio. As a further check on data accuracy, solid samples were collected at the same condition by simply closing the isolation valves and removing the filter. The filter was a Balston P/N 100-25-DH, housed in a Balston filter holder, type 30/25.

For reference, the sampling probe was manufactured from stainless steel pipe, 3.18-cm (1.25-in) diameter, 4.76-mm (0.188-in) wall thickness. The central tube, which conveys the sample, was made from 9.53-mm (0.375-in) stainless tubing, with the remaining annuli constructed from 19.1-mm (0.75-in) and 12.7-mm (0.50-in) stainless steel tubing. The probe tip was machined from a solid stainless steel billet and then welded to the tubes such that the welds were in contact with cooling water. An earlier probe design was revised because welded junctions at the very tip of the probe repeatedly failed from thermal stress.

4.0 Test Characterization and Sorbent Injection

Earlier investigations of the super-equilibrium process (Abichandani, Chatwani, and Stickler 1989; Bannister et al. 1990) suggested that a number of factors would be essential to rapid sulfur capture:

- High temperatures. At the outset of this work, discussions with investigators at AVCO Research Laboratory suggested that 1,920 K (3,000 °F) would be a minimum gas temperature required to initiate the rapid sulfur capture process.

- Rapid mixing of the sorbent with the hot gases. To promote rapid mixing, a "mixing block" was installed in the transition between the jet-stirred and plug-flow zone of the GTRC as shown in Figure 6.

The mixing block was formed from the same castable refractory as the rest of the combustor interior. The water-cooled sorbent injection probe enters the center of the mixing block at a right angle to the four radial passages, through which the hot gas exits the jet-stirred zone and enters the plug-flow zone. This geometry creates four jets, which mix the incoming sorbent stream.

The sorbent injection probe was constructed from a co-annular series of tubes, with a 4.8-mm (0.19-in) inside diameter (i.e., constructed from 6.35-mm [0.25-in] stainless tube, 0.035-inch wall). Cooling water circulated through the outer annuli, and a formable refractory (Fiberfrax, Carborundum Co.) coated the outside of the probe to prevent heat loss from the jet-stirred region.

Shakedown tests verified that the mixing block did thoroughly mix the sorbent with the hot gases. Temperature profiles were taken along the axis of the plug-flow region, both with and without the sorbent carrier gas. When the carrier gas mixed ideally with the products of the jet-stirred zone, the temperature profile with the carrier gas was parallel to the case without the carrier gas, except shifted lower by the sensible heat absorbed by the carrier nitrogen.

Temperature measurements of this kind must account for the radiation error associated with thermocouple measurements in hot gases. Toward this end, a suction pyrometer was built as shown in Figure 7. (Dimensions of the metal tubing are the same as those for the gas sampling probe, which are discussed at the end of section 3.3. Dimensions of the alumina radiation shield are as shown in Figure 7.) Combustion gases flow at high velocity across the type-R thermocouple junction and through the 12 holes in the surrounding ceramic. The thermocouple junction is coated with refractory glue and located at the end of the two-conductor insulating rod. Calculations of the bead temperature at representative flow rates showed that, at 10 atmospheres pressure and 2,000 K (3,140 °F), this pyrometer would measure a temperature of more than 1,990 K (3,122 °F) when the wall temperature was 1,800 K (2,780 °F).

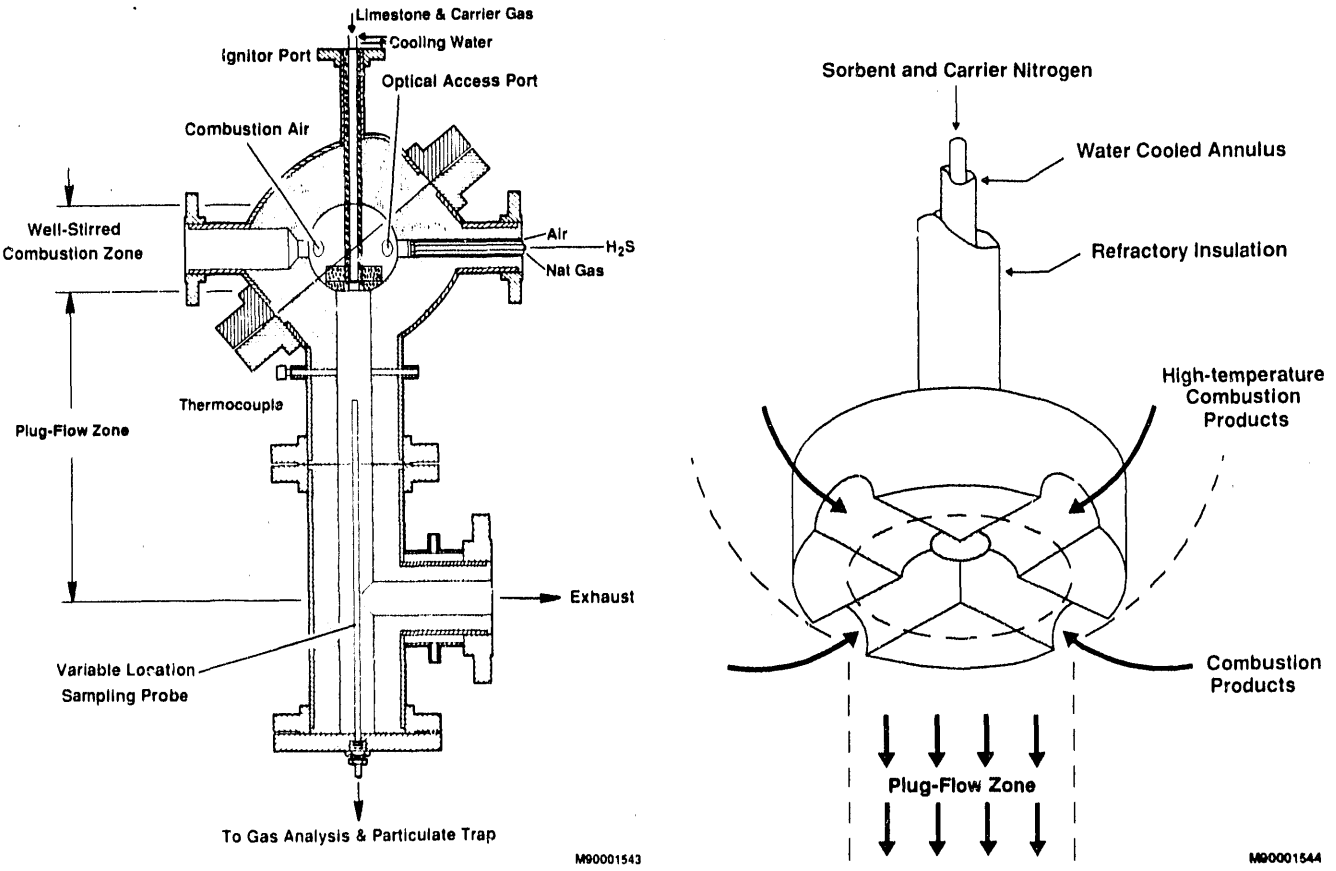

Figure 6. Mixing Block Geometry and Sorbent Injection Approach

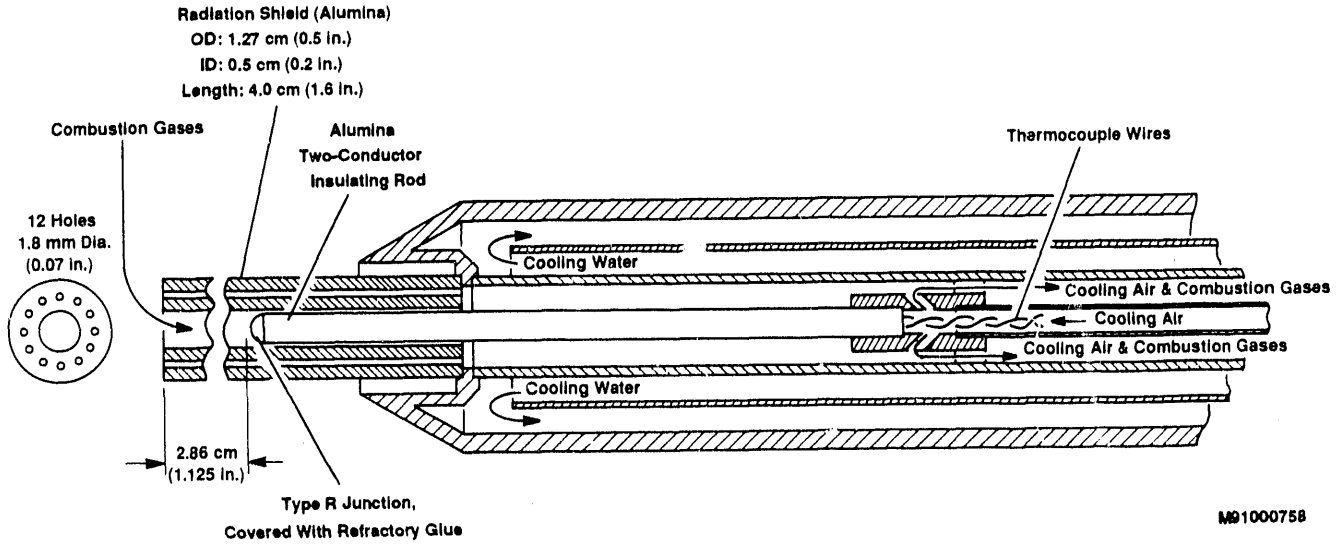

Figure 7. Suction Pyrometer Detail

The suction pyrometer was tested by steadily increasing the flow across the junction until further increases in flow did not produce a temperature rise. Extreme care was needed to control the flow, since a proper ratio of combustion flow to the cooling nitrogen was essential to keep the thermocouple wire insulation from melting in the lower portions of the probe. Typical operating conditions were 2.8 g/s (300 scf/h) cooling nitrogen and 0.94 g/s (100 scf/h) sample flow.

Using the suction pyrometer, two temperature profiles were produced (Figure 8). Operating conditions for these profiles are shown below the figure. The upper curve represents the temperature profile without the sorbent carrier gas, the lower curve with the sorbent carrier gas. Several features are evident from these data. First, the curves are parallel as expected, indicating that the mixing is very complete. Second, there is a reduction in temperature of approximately 55 K (100 °F) along the plug-flow zone caused by heat loss. Note that these data were collected on the lean side of stoichiometric (equivalence ratio 0.83), so higher peak temperatures were achieved closer to stoichiometric; these curves do not represent the maximum temperatures in the experiment.

Shakedown tests of the sorbent injection system were conducted as part of the initial attempts to obtain sulfur capture data. The sorbent injection probe clogged rapidly at the tip near the mixing block. The clog was detected by a rapid increase in the sorbent feed tank pressure, which was usually operated at 962 kPa (140 psig). During normal operation, the feed tank pressure would climb about 14 kPa (2 psi) during the nominal 5 minutes when sorbent was fed into the combustor. Turning the sorbent feeder off would then return the tank to its original pressure. A clogged injection probe could be identified by a rise in pressure of more than 14 kPa, coupled with a failure to return to normal operating pressure after the feeder was shut off.

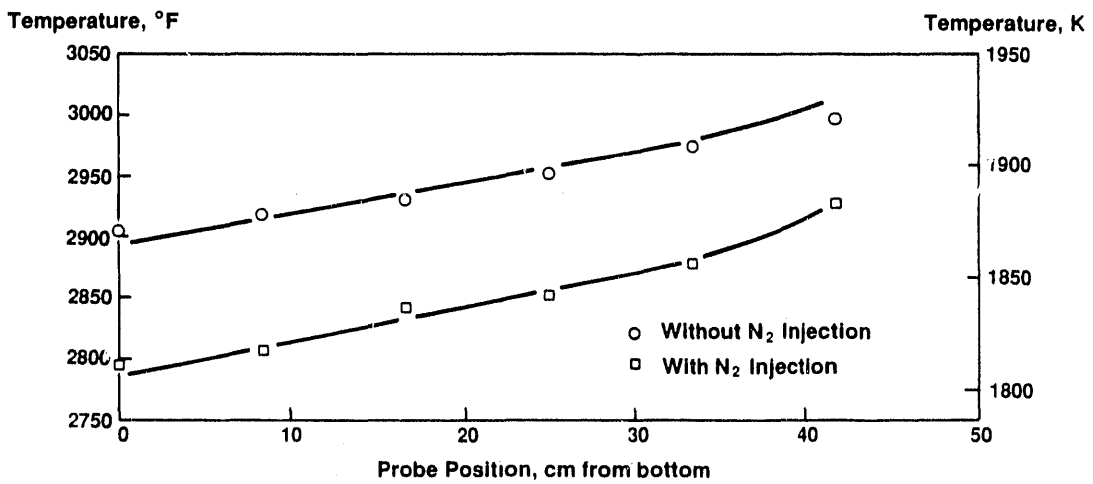

Figure 8. Temperature Profiles

During initial tests, injector plugging was frequent and severe. Plugs could seldom be cleared using pressurized nitrogen on the feed line opened at the shutoff valves (Figure 4). This problem was eventually traced to the water-cooled injector probe. The plugging was the result of the water-cooled tip at the end of the injector probe, which was allowing some water condensate (from the products of combustion) to form on the metal surface. This water captured and retained limestone, eventually bridging the opening. To eliminate this problem, a section of 9.5-mm (0.375-in) stainless steel tubing that was 6.4 millimeters (0.25 inches) in length was welded to the end of the probe. The additional tube was heated by the combustion environment to temperatures above the liquid dewpoint, thereby preventing the condensate that led to plugging. As a further protection, the interior of the tube was coated with refractory cement to allow a high enough surface temperature to prevent condensation. Subsequent operation was steady without serious plugging problems.

Initial tests identified some potentially difficult problems, which were subsequently resolved. The plug-flow interior was being melted by interactions with the limestone, a problem somewhat expected from earlier discussions with Professor J. Brown at Virginia Polytechnical Institute. Brown noted that the chosen refractory was among the best for this application, but warned that some initial melting could be expected until a coating had formed over the refractory. In fact, this is what happened; the plug-flow zone was eventually coated with a hard, glassy material. While acceptable for the plug-flow walls, this behavior led to aggravating problems with the mixing block (Figure 6). Because the mixing block was susceptible to melting when limestone was present, the block was often deformed during the test. In a number of tests, molten refractory dripped from the mixing block into the sampling probe, immediately plugging it.

As a result, tests were conducted without the mixing block, both at stoichiometric and on the rich and lean side of stoichiometric. Comparison of data to earlier results with the mixing block showed no discernable effect on sulfur capture. Depending on the operating conditions, some measured non-uniformity in the temperature profile near the top of the plug flow typically produced a 55 K (100 °F) reduction in temperature near the top of the plug-flow region.

5.0 Test Procedures

Testing proceeded as follows:

1. Establish the desired operating conditions for all gaseous flows, but leave the sorbent feeder off. Time required was approximately 3 to 5 hours to establish temperature and flow rates and calibrations.

2. At operating conditions, turn on the sorbent feeder for 2 to 5 minutes, then turn it off and recover the solid sample from the filter holder (Figure 5).

3. Between runs, inspect and repair refractory surfaces and clean sample lines. Maintenance time between runs was typically 1 to 2 days.

Unless stated otherwise, certain parameters were held constant throughout these tests: 10 atmospheres pressure; molar calcium:sulfur ratio of 1:1; and gas phase sulfur level at 3,000 ppmv.

A typical test produced three to five data points. Temperatures reported for the tests were computed in the following manner:

- Early tests showed that the difference between the calculated adiabatic temperature and the temperature measured at several equivalence ratios was nearly constant.

- After the sulfur tests were complete, temperatures were measured using the suction pyrometer at the probe position corresponding to the 30-ms residence time, at the same total airflow as in the majority of the tests.

- The difference between the adiabatic temperature and the temperature measured at this point was used to correct the calculated temperature for heat loss.

- Temperatures at any condition of interest were thus determined by subtracting the same constant value 264 K (475 °F) from the adiabatic flame temperature calculated using the CEC code.

6.0 Results

Testing began by looking for conditions where "super-equilibrium" sulfur capture occurred. The sorbent was -200 mesh Germany Valley limestone purchased locally and sieved on site. This limestone was selected based on published reports, which indicated it to be a relatively active sorbent for sulfur capture (Fee et al. 1980). The composition analysis of the limestone is shown in Table 1.

Table 1. Composition Analysis of Germany Valley Limestone

Element	wt %
Ca	31.0
K	< 0.01
Na	< 0.01
Fe	0.045
Mg	0.740
Mineral C	11.7
S	< 0.01

Recognizing the importance of temperature in the sulfur capture process, data were acquired over a range of equivalence ratios and, hence, temperatures at 30-, 50-, and 70-ms residence times. The results of these tests are shown in Figures 9, 10, and 11.

Utilization values come from on-line gas analysis and from off-line solids analysis. The bulk of the data was acquired at stoichiometric or fuel-lean conditions; the four solids data points were acquired at fuel-rich conditions with equivalence ratios less than 1.2. A few tests were conducted with -325 mesh limestone, but no significant difference was observed; therefore, these data points are simply included with the others.

Finally, attempts to use the mixing block were eventually frustrated because it would melt and drip into the sampling probe, clogging the sampling train. Again, no significant difference was observed with or without the mixing block present; therefore, no distinction is made on the plots.

The data show some consistent trends. First, all three residence times show reduced sulfur capture as temperature increased, for both the gas analysis and the solids analysis. The agreement between gas and solids analysis is good at the short residence time (30 milliseconds), but is worse at the 50- and 70-ms residence times, especially at low temperatures.

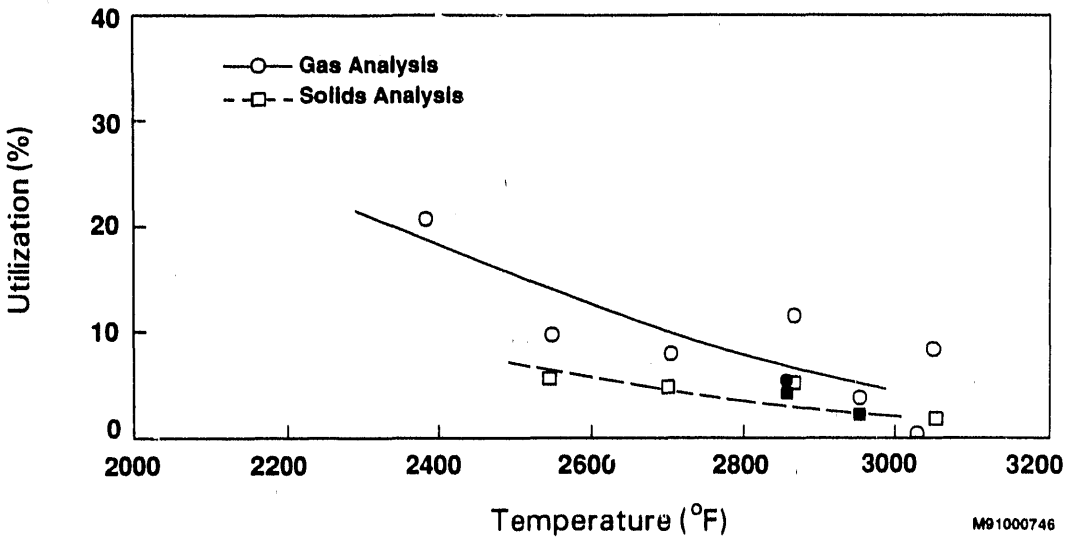

Figure 9. Sulfur Capture Data at 30-ms Residence Time

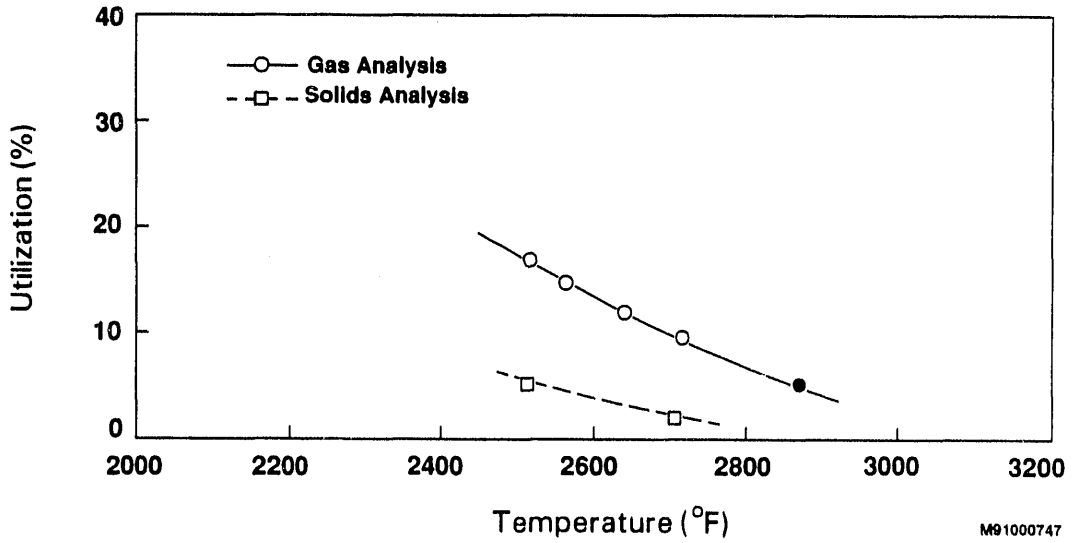

Figure 10. Sulfur Capture Data at 50-ms Residence Time

Second, utilization as measured from the gas analysis was typically higher than that recorded from solids analysis. This behavior is thought to occur because gas samples will include gases that can be scrubbed of sulfur by sorbent flowing adjacent to the cooler walls of the plug flow. (This is shown schematically in Figure 12.) If the sorbent and gases flow straight down the plug-flow section, sorbent near the cooler walls may be able to absorb some sulfur by traditional equilibrium mechanisms. Additional sulfur gases will then diffuse across

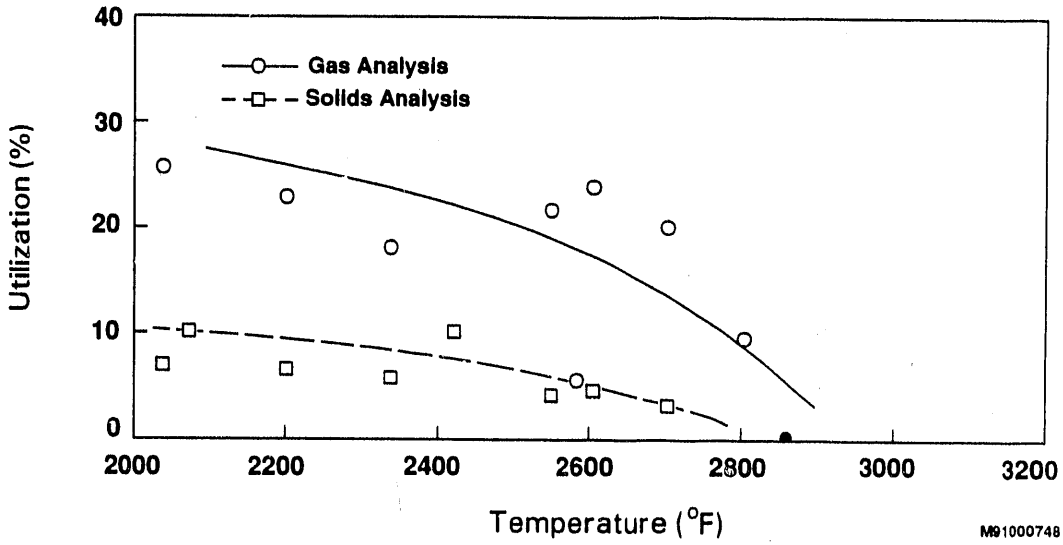

Figure 11. Sulfur Capture Data at 70-ms Residence Time

the region from the core of the plug-flow zone, lowering the measured gas concentration of sulfur species. However, particles that are sampled as they travel down the centerline of the reactor experience hotter temperatures than those near the wall; therefore, they capture less sulfur.

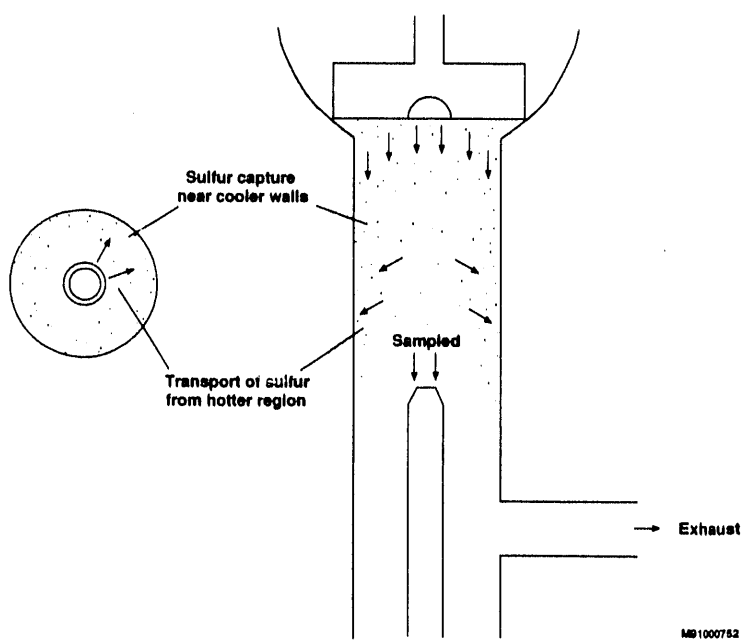

Figure 12. Sulfur Capture Behavior in the Plug-Flow Region of the GTRC

While this hypothesis is undoubtedly complicated by turbulent transport of the sorbent across the region, it should predict the following behavior: higher gas temperatures and shorter residence times produce closer agreement between the gas and solids analysis. For example, if the gas temperature is high enough, then even the particles in the cooler wall regions would still be heated above the point where equilibrium favors sulfur capture. Such behavior is evident in the data. Perhaps the most significant point to note about the data is that the agreement between gas analysis and solids analysis is good at short residence times. This agreement addresses the extent of mixing either with or without the mixing block.

It was hypothesized that the relatively low levels of sulfur capture resulted from the mixing block (or even the combustor geometry without the mixing block) creating swirl sufficient to distribute most of the sorbent against the wall of the reactor, effectively extending the residence time. If this were so, the gas sample from the shortest residence time would not agree with the solid sample, because the core of the flow would be deficient in sorbent. One would expect the results of the gas analysis to be less than the solids analysis early in the plug-flow zone and later to become equal. To the contrary, however, the best agreement was obtained at the shortest residence times.

The few data points that were obtained under fuel-rich conditions were not significantly different from those obtained at fuel-lean or stoichiometric operation. This similarity is especially evident in the 30-ms data, where a number of overlapping data points were obtained at nearly the same temperature but at rich and lean stoichiometries.

Figure 13 plots limestone calcination against temperature, at 30- and 70-ms residence times, and for -200 mesh limestone. The data are consistent with expected behavior below 1,756 K (2,700 °F). Below this temperature, the longer residence time shows consistently higher calcination, and the extent of calcination increases with increasing temperature. However, above 1,756 K (2,700 °F), the 30-ms data appear to drop with temperature. Even a pessimistic discard of the extreme data points above this temperature would still show the curve leveling off, if not dropping. Such behavior can only be explained by the activation of mechanisms that inhibit the calcination reaction, such as sintering of the particle exterior. More study would be needed to draw definite conclusions, but it is interesting to note that for the Milne and Pershing (1988) model, calcination and sintering reactions with Arhenius kinetics have activation energies of 22 kcal/mol and 60 kcal/mol, respectively. The implication is that the sintering reaction rate is sensitive to temperature and could surpass the calcination rate at high temperatures.

These data show that sulfur capture is relatively small at conditions that were thought to be of interest for super-equilibrium sulfur capture. To ensure that this result was not peculiar to the chosen limestone, reagent grade calcium carbonate (RGCC) was used for the next sorbent tests. Similar sorbent was used in earlier studies at AVCO and produced the super-equilibrium behavior.

The RGCC was smaller than the sieved limestone, with almost 90% of the particles less than 10 micrometers (volume basis, from coulter counter measurements). The relatively small particle sizes suggested that data should be acquired at short residence times since smaller particles would heat and react sooner. Thus, the precipitated limestone was tested at 15-, 18-, and 30-ms residence times. These tests were difficult, because the precipitated limestone rapidly clogged the conveying feed line between the sorbent feeder vessel and the GTRC. The feeding difficulty resulted in on-line, gas sample measurements of dubious value, since a clogging feed line would lower the sorbent feed rate, producing an artificially low calcium to sulfur ratio, and consequently little change in the gaseous sulfur level. However, such difficulties would not affect the measured sulfur capture in the solids samples collected from the reactor. Three data points were obtained at a temperature of 1,956 K (3,060 °F), corresponding to an equivalence ratio of 0.95.

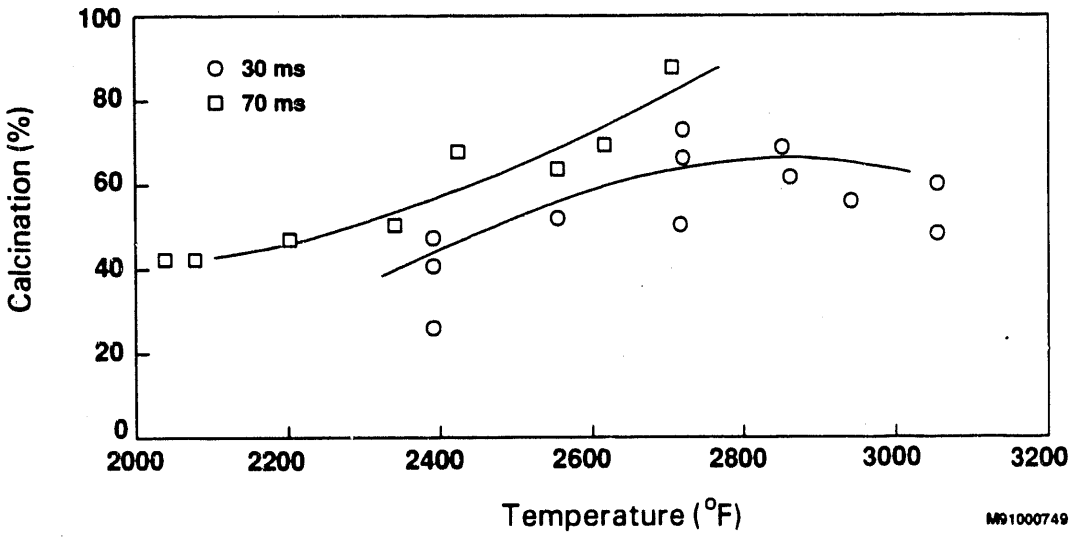

Figure 13. Calcination Data for -200 Mesh Germany Valley Limestone

Sorbent utilization and calcination are plotted for the RGCC test in Figure 14. Again, utilization is low, less than 11%. Calcination is near 50%, indicating that even at the 15-ms test point, significant particle heating has occurred. Surprisingly, little increase in calcination is observed between 18 and 30 ms.

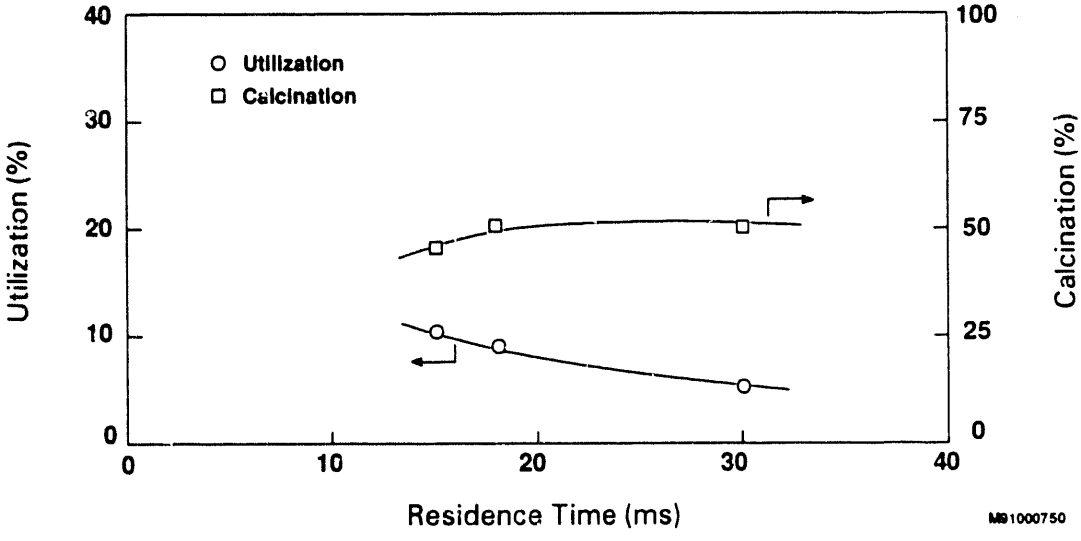

Figure 14. Results for Reagent Grade Calcium Carbonate (RGCC)

Photographs of the precipitate samples collected at residence times of 18 and 20 ms support the unexpected behavior of the calcination plotted versus residence time at constant temperature. Shown in Figure 15 is a sample of the RGCC sorbent used in the tests. The photo of the precipitate at 18 ms (Figure 15B) shows little visible change with respect to the original limestone sorbent in Figure 15A. The photo of the precipitate at 30 ms (Figure 15C), however, shows a radical difference, with obvious sintering of the sorbent particles. Note that Figures 15A and 15B are photos at the 1-micrometer scale, while the photo in Figure 15C is at the 10-micrometer scale.

The Germany Valley sorbent exhibited behavior similar to that of the RGCC sorbent. The original Germany Valley limestone sample and the precipitate at a residence time of 30 ms and a temperature of 3,060 °F are shown in Figure 16. Figure 16A, the photo of the original Germany Valley sample, is at the 1-micrometer scale, while Figure 16B, the photo of the precipitate at 30 ms, is at the 10-micrometer scale. Comparison of the two photos shows convincingly that sintering occurred to a large degree in the Germany Valley sorbent as in the RGCC sorbent. The photos also support the proposed competition between calcination and sintering suggested by the data in Figure 13, which illustrates the apparent decrease in the extent of calcination above 1,756 K (2,700 °F) at short residence times. Although sintering is observed in the photographs, calcination is appoximately 50 percent complete (Figure 13), suggesting that the two processes are occurring at comparable rates.

The data presented thus far fail to demonstrate appreciable sulfur capture. Many on-line attempts were made to define conditions that would promote sulfur capture. By moving the sampling probe, changing the equivalence ratio, and adjusting the sorbent or sulfur flow rate, it was possible to quickly scan a range of parameters and seek an appreciable change in the gaseous sulfur concentration. No conditions were found that produced the high levels of sulfur capture predicted in the super-equilibrium concept.

To investigate a few remaining possibilities, a test of the effect of calcium-to-sulfur ratio was conducted. The test was performed in two ways using the standard -200 mesh Germany Valley Limestone. First, the sulfur level was reduced from the nominal 3,000 ppmv to 1,500 ppmv, while maintaining the same sorbent flow rate. This resulted in a 2:1 Ca/S ratio. Then, the sorbent flow was increased by a factor of 2, producing a 4:1 Ca/S ratio. Finally, the sulfur level was increased to 3,000 ppmv, producing a Ca/S ratio of 2:1. Results from the test are presented in Table 2.

Comparing the magnitude of utilization and calcination with earlier results, it is clear that the higher Ca/S ratios do not significantly change sorbent performance. As might be expected, the reduced sulfur concentration leads to a reduced utilization. This is seen directly in Figure 17, where the data from Table 2 having a Ca/S ratio of 2:1 and 1,500 ppmv sulfur are plotted with earlier data having a Ca/S ratio of 1:1 and initial sulfur levels of 3,000 ppmv.

The data show reduced utilization at the lower sulfur level of 1,500 ppmv, as might be expected. Note that the last data point in Table 3, having a Ca/S ratio of 2:1 but an initial sulfur level of 3,000 ppmv, fits in well with the other data at a Ca/S ratio of 1:1 and

Figure 15A. RGCC Sorbent Reagent Grade $CaCO_3$, Unreacted

Figure 15B. RGCC Sorbent Precipitate at 18 ms

Figure 15C. RGCC Sorbent Precipitate at 30 ms

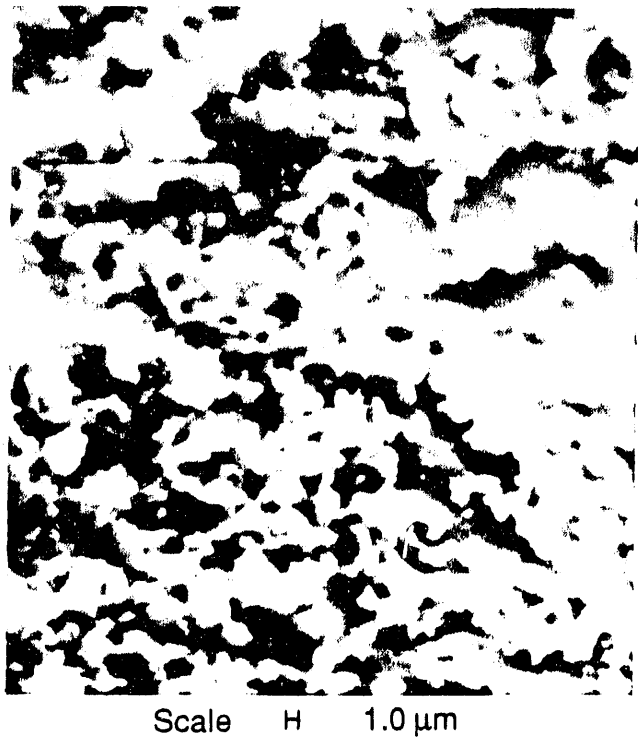

Figure 16A. Germany Valley Limestone Sieved, Unreacted

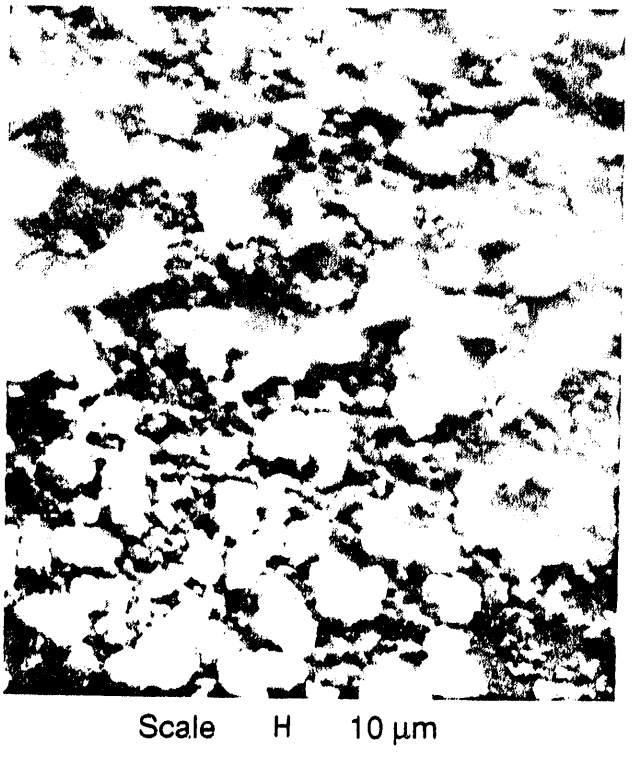

Figure 16B. Germany Valley Limestone Precipitate at 30 ms

3,000 ppmv sulfur. In other words, higher sulfur levels promote better utilization at these conditions; the Ca/S ratio is less important.

In addition to the measurements discussed thus far, the data listed in Table 2 also include surface area measurements of the sorbent as determined by nitrogen adsorption. The measured surface areas are disappointingly low.

As noted below the chart, the original Germany Valley Limestone had a surface area of 2.02 m^2/g before reaction. It was expected that reasonable sulfur capture levels would require surface areas of at least 50 m^2/g, considerably higher than the measured values. The low surface areas must certainly contribute to the low utilization measured here. It is not clear why surface areas were not higher. One cannot argue that the sorbent particles were not rapidly heated, because the calcination data clearly show that calcination is well underway at the 30-ms residence time. In addition, higher temperatures significantly affect the extent of calcination, yet do not affect the surface area. The low surface areas may be the result of sintering; this would be consistent with the earlier discussion regarding Figures 15 and 16, but one might then expect that lower temperatures should produce higher surface areas, which is

Table 2. Sulfur Capture at Ca/S Ratios Other Than One
(30-ms Residence Time)

Equivalence Ratio	Temperature (°F)	Ca/S Mole Ratio	Sulfur Concentration (ppmv)	Utilization (%)	Calcination (%)	Surface area (m^2/g)
0.72	2,384	2	1,500	2.29	21.4	2.19
0.83	2,705	2	1,500	2.54	50.3	2.61
0.98	3,060	2	1,500	0.91	60.9	2.82
0.72	2,384	4	1,500	3.77	40.5	3.17
0.72	2,384	2	3,000	5.55	47.2	2.95

Notes: Calcination and utilization data are from solids analysis.
Surface area from nitrogen adsorption isotherm.
Initial surface area before reaction: 2.02 m^2/g.

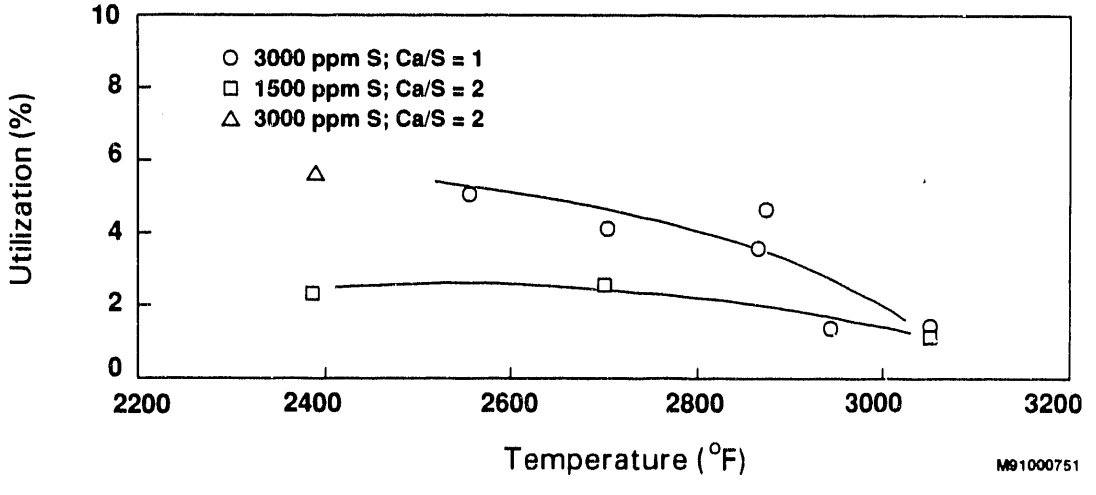

Figure 17. Utilization With Various Ca/S Ratios and Sulfur Levels

not observed in the data. To ensure that the low surface areas were not peculiar to the Germany Valley Limestone, the RGCC samples were also measured for surface area. The results, presented in Table 3, show that the measured surface areas are low, not differing significantly from the original values. These low surface areas were measured in spite of relatively high levels of calcination in progress.

Table 3. Surface Area Data for the Reagent Grade Calcium Carbonate

Residence time (ms)	Surface area (m^2/g)
15	15.4
18	10.8
30	7.2

Note: Initial surface area: 10.9 m^2/g.

7.0 Summary

The data presented have failed to demonstrate significant sulfur capture under conditions that were thought to have favored the rapid sulfur capture process. Variations in residence time, temperature, Ca/S ratio, sulfur concentration, and sorbent type were all investigated, yet no conditions were found that produced a sulfur capture of more than a few percent. Sulfur capture was lower as the gas temperature approached 1,922 K (3,000 °F), the opposite of the behavior anticipated based on the work of Abichandani, Chatwani, and Stickler (1989) and Bannister et al. (1990).

Data on surface area and calcination showed some interesting trends. Although these trends may be of fundamental interest, without appreciable sulfur captures, they did not merit further study in the present test series.

8.0 References

Abichandani, J.S., A.U. Chatwani, and D.B. Stickler. 1989. *Super-Equilibrium Sulfur Removal From High-Temperature Gases.* DOE/MC/23262-2783. NTIS/DE90000437. Springfield, Va.: National Technical Information Service.

Bannister, R.L., P.W. Pillsbury, R.C. Diehl, and P.J. Loftus. 1990. Recent Test Results in the Direct Coal-Fired 80 MW Combustion Turbine Program. Paper presented at ASME Gas Turbine and Aeroengine Congress and Exposition, June 11-14, Brussels, Belgium, ASME Paper No. 90-GT-58.

Borgwardt, R.H. 1985. Calcination Kinetics and Surface Area of Dispersed Limestone Particles. *AIChE Journal* 31:103-111.

Chadaille, J., and Y. Braud. 1972. Measurements in Flames. In *Industrial Flames, Volume 1*, ed. J.M. Beer and M.W. Thring, 95-162. Edward Arnold Publishers.

Fee, D.C., W.I. Wilson, J.A. Shearer, G.W. Smith, J.F. Lane, L.-S. Fan, K.M. Myles, and I. Johnson. 1980. *Sorbent Utilization Prediction Methodology: Sulfur Control in Fluidized-Bed Combustors.* Argonne National Laboratory Report. ANL/CEN/FE-80-10.

Gordon, S., and B.J. McBride. 1976. *Computer Program for Complex Chemical Equilibrium Composition, Incident and Reflected Shocks, and Chapman Jouget Detonations.* rev. ed. NASA SP-273.

Lawson, W.F., D.J. Maloney, D.W. Shaw, G.A. Richards, R.J. Anderson, J.M. Cook, R.V. Siriwardane, J.A. Poston, and M.A. Colaluca. 1990. Investigation of Rapid Sulfur Capture. In *Proceedings of the Seventh Annual Coal-Fuel Heat Engines and Gas Stream Cleanup Systems Contractors Review Meeting*, 283-292. DOE/METC-90/6110. NTIS/DE90000480. Springfield, Va.: National Technical Information Service.

Milne, C.R., and D.W. Pershing. 1988. *An Experimental Study of the Fundamentals of the SO_2/Limer Reaction at High Temperatures.* AEERL-P-457, R9/26/88.

913546

END

DATE FILMED

12/27/91